Energy and Centrality Dependence of Deuteron and Proton Production in Pb+Pb Collisions at CERN-SPS

T. Anticic[21], B. Baatar[9],D. Barna[5], J. Bartke[7], R.A. Barton[3], M. Behler[15], L. Betev[10], H. Białkowska[19], A. Billmeier[10], C. Blume[8], C.O. Blyth[3], B. Boimska[19], M. Botje[1], J. Bracinik[4], R. Bramm[10], R. Brun[11], P. Buncic[10,11], V. Cerny[4], O. Chvala[17], G.E. Cooper[22] , J.G. Cramer[18], P. Csató[5], P. Dinkelaker[10], V. Eckardt[16], P. Filip[16], H.G. Fischer[11], Z. Fodor[5], P. Foka[8], P. Freund[16], V. Friese[8,15], J. Gál[5], M. Gaździcki[10], G. Georgopoulos[2], E. Gładysz[7], S. Hegyi[5], C. Höhne[15], G. Igo[14], P.G. Jones[3], K. Kadija[11,21], A. Karev[16], V.I. Kolesnikov[9], T. Kollegger[10], M. Kowalski[7], I. Kraus[8], M. Kreps[4], M. van Leeuwen[1], P. Lévai[5], A.I. Malakhov[9], S. Margetis[13], C. Markert[8], B.W. Mayes[12], G.L. Melkumov[9], C. Meurer[10], A. Mischke[8], M. Mitrovski[10], J. Molnár[5], J.M. Nelson[3], G. Pálla[5], A.D. Panagiotou[2], K. Perl[20], A. Petridis[2], M. Pikna[4], L. Pinsky[12], A.M. Poskanzer[22], F. Pühlhofer[15], J.G. Reid[18], R. Renfordt[10], W. Retyk[20], C. Roland[6], G. Roland[6], A. Rybicki[7], T. Sammer[16], A. Sandoval[8], H. Sann[8], N. Schmitz[16], P. Seyboth[16], F. Siklér[5], B. Sitar[4], E. Skrzypczak[20], G.T.A. Squier[3], R. Stock[10], H. Ströbele[10], T. Susa[21], I. Szentpétery[5], J. Sziklai[5], T.A. Trainor[18], D. Varga[5], M. Vassiliou[2], G.I. Veres[5], G. Vesztergombi[5], D. Vranić[8], S. Wenig[11], A. Wetzler[10], C. Whitten[14], N. Xu[22], *I.K. Yoo*[8,15], J. Zaranek[10], J. Zimányi[5]

(The NA49 collaboration)

[1] *NIKHEF, Amsterdam, Netherlands.*
[2] *Department of Physics, University of Athens, Athens, Greece.*
[3] *Birmingham University, Birmingham, England.*
[4] *Comenius University, Bratislava, Slovakia.*
[5] *KFKI Research Institute for Particle and Nuclear Physics, Budapest, Hungary.*
[6] *MIT, Cambridge, USA.*
[7] *Institute of Nuclear Physics, Cracow, Poland.*
[8] *Gesellschaft für Schwerionenforschung (GSI), Darmstadt, Germany.*
[9] *Joint Institute for Nuclear Research, Dubna, Russia.*
[10] *Fachbereich Physik der Universität, Frankfurt, Germany.*
[11] *CERN, Geneva, Switzerland.*
[12] *University of Houston, Houston, TX, USA.*
[13] *Kent State University, Kent, OH, USA.*
[14] *University of California at Los Angeles, Los Angeles, USA.*
[15] *Fachbereich Physik der Universität, Marburg, Germany.*
[16] *Max-Planck-Institut für Physik, Munich, Germany.*
[17] *Institute of Particle and Nuclear Physics, Charles University, Prague, Czech Republic.*
[18] *Nuclear Physics Laboratory, University of Washington, Seattle, WA, USA.*
[19] *Institute for Nuclear Studies, Warsaw, Poland.*
[20] *Institute for Experimental Physics, University of Warsaw, Warsaw, Poland.*
[21] *Rudjer Boskovic Institute, Zagreb, Croatia.*
[22] *Lawrence Berkeley National Laboratory, Berkeley, CA, USA.*

(DRAFT of March 2003)

In the NA49 experiment at the CERN SPS the transverse mass m_t-distributions for deuterons and protons (corrected for feeddown from weak hyperon decays) are measured in Pb+Pb reactions near midrapidity and in the range $0 < m_t - m < 1.0(1.5)$ GeV/c^2 for a wide range of the collision centrality at 158 AGeV and for the 7% most central collisions at 40 and 80 AGeV beam energies.

The rapidity density dn/dy and inverse slope parameter T derived from m_t-distributions as well as the coalescence parameter B_2 (ratio d/p^2) are studied as a function of the incident energy and the collision centrality. The deuteron m_t-spectra are significantly harder than those of protons, especially in cental collisions. The coalescence factor B_2 shows a strong decrease with increasing centrality reflecting enlargement of the particle emission source in central Pb+Pb collisions. Moreover, the B_2 exhibits a trend to increase with increasing m_t. Also, the B_2 shows a steadily increase with decreasing incident energy even within the SPS energy range. The results are discussed and compared to the predicted characteristics of the models that explicitly include the strong collectve expansion of the source created in Pb+Pb collisions.

I. INTRODUCTION

For studying the evolution of the nuclear systems created in relativistic heavy ion collisions the emitted hadrons, in particular the protons and light nuclei, are widely employed [1]. There is a great deal of evidence that in early stage of high energy nucleus-nucleus collisions the nuclear matter is highly compressed and hot reaching the energy densities an order of magnitude greater than that of normal nuclear matter. With the time, this system (fireball) expands and cools, and the interaction among the particles almost ceases. This is the latest time of the evolution of the fireball, called the stage of freeze-out, when a fragile light nuclei, in particular deuterons, near center-of-mass rapidity are formed. Due to their small binding energy it is very probably they will not survive repeated collisions inside the fireball and they are also unlikely to be the fragments of projectile or target because of the violence of heavy ion collisions. Thus, the observed deuterons are believed to be created by coalescence via correlation of protons and neuterons at freeze-out.

In general, the coalescence models relate the invariant yield of light nuclei with mass A to the A-th power of the proton yield [2], assuming the neuteron and proton distributions are identical :

$$E_A \frac{d^3N_A}{dp_A^3} = B_A \left(E_p \frac{d^3N_p}{dp_p^3}\right)^A, \quad p_A = A \cdot p_p, \qquad (1)$$

The coalescence factor B_A, which characterizes the coalescence probability, depends on the nucleon density in the fireball and thus on its size as well as on its internal dynamics , it may be measured in the experiment and used for estimation of the reaction volume that is creating the composite partcles. Several prescriptions were proposed to calculate a source radius based on B_A parameter, where the coalescence parameter scaled with the reaction volume as $B_A \propto (1/V)^{A-1}$ [3–5].

Originally, the simple momentum space coalescence models [6], which assumed a coalescence to take place between any nucleons with a small momentum difference, successfully described an early measurements of the light nuclei production in A-A collisions at Bevalac and SIS energies of 0.2-2.0 AGeV [7,8] as well as in high energy p+p and p+A collisions at FNAL [9]. Under the assumption of a constant B_A the coalescence relation explains the yields of light nuclei in above experiments and the independence of B_A on the beam energy and the size of colliding nuclei, as well as on the transverse momentun and rapidity was regarded as a scaling behaviour [2].

However, at the typical AGS energies of 10-15 AGeV [10–14] and at 158 AGeV at CERN [15–17] the B_A was found to be, at least, an order of magnitude smaller, and this observation was attributed to the larger source volume due to hydrodynamic expansion of the collision zone before freeze-out. This approach was developed in thermal and density matrix coalescence models [4,5], which considered a significant expansion in the collision volume, albeit no correlations between position and momentum of the nucleons were considered in their presentation. However, the presence of collective motion(flow) leads not only to expansion of the collision volume but also signoficant position-momentum correlations between particles at freeze-out affecting the process of cluster formation [29,37]. Indeed, the overall expension of the system tends to reduce the coalescence probability B_A spatially isolating(separating) nucleons from each other, whereas the collective flow, in contrary , increases B_A affecting in the oposite direction, it makes more likely for nucleons being close in configuration space to have also similar momenta and to make easier cluster formation.

The advanced coalescence models [18–20] have recently been developed for the systems with strong collective expansion including the effects both larger source volume and collective motion. A theoretical analysis [18,19] has found that the inverse slope systematics and the m_t-dependence of B_A arise from an interplay of transverse flow and the radial dependence of the nucleon density, and their functional discription have been predicted . In this context, the experimantal study of the light nuclei production at various beam energy, collision centrality and transverse mass of emitted particles is great of importance since it possibly might be used to disentangle above competing effects governing the nuclear cluster formation.

II. EXPERIMENTAL METHOD

The experiment was carried out with the NA49 large acceptance hadron detector [21] using external ^{208}Pb ion beams with energies of 40, 80 and 158 GeV/nucleon produced by the CERN SPS. Charged particles emitted from collision with a Pb target of 224 mg/cm^2 in thickness (equivalent to 1% interaction length) are detected over a large fraction of a phase space by tracking in four large volume Time Projection Chambers (TPCs). Two of them (Vertex TPCs) are located in magnetic field and two others (Maim TPCs) are placed behind the magnet on either sides of the beam line. Particle momentum and velocity are determined from tracking through magnetic field and measuring the specific energy loss dE/dx in the TPC gas with a resolution of about 4%. Two 2.2 m^2 time-of-flight walls (TOF) containing 891 scintillator pixels each are symmetrically situated behined the Main TPCs on both sides of the beam. The overall time resolution is $60-70$ ps. In this work, the identification of protons and deuterons were primarily accomplished by the TOF measurement, augmented by dE/dx information from TPCs which provides substantial elimination of a vast source

of background coming from charged pions and kaons. A particle identification capability is demonstrated in Fig.1.

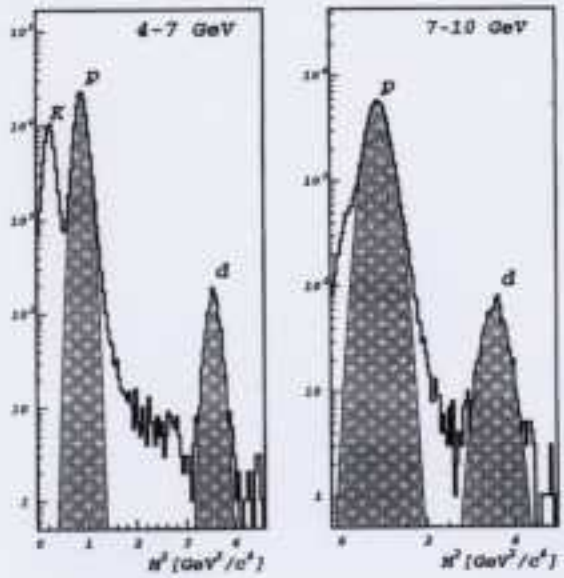

FIG. 1. a) Invariant mass spectra for particles at the momenta p=4-7 GeV/c and p=7-10 GeV/c. The Gaussian fit to the proton and deuteron mass peaks are shown as a shaded area.

Online event characterization and triggering is accomplished by beam definition detectors located in the beam line upstream of the target and interaction counters and calorimeters downstream of the target. The data samples were recorded with two trigger settings, providing selection of the central and minimum bias events.

For central Pb+Pb collisions, the primary trigger detector is a zero degree calorimeter (ZDC) located downstream of the target behind a collimator, which measures the energy remaining in the projectile fragments traveling forward as well as the beam particles and specrator protons, neuterons traveling forward into the calorimeter. The upper limit on the energy in ZDC was set to accept the 12% most central events at 158 AGeV and 7% at 40 and 80 AGeV from all inelastic Pb+Pb collisions.

In the measurements of the minimum bias Pb+Pb collisions, the Cherenkov counter is used to detect the Cherenkov light produced by non-interacting projectiles or fast secondary particles in the gas region immediately behind the target in order to veto these events. Triggering is accomplished by placing an upper threshold on the signal from this Cherenkov counter in coincidence with valid signal from the beam detectors. Additionally, the offline cuts on the z-position of the fitted primary vertex were made to limit the fraction of the non-target background events while minimizing the bias imposed against peripheral events.

III. DATA ANALYSIS AND RESULTS

For the present study of 158 AGeV Pb+Pb collisions 320,000 central and 735,000 minimum bias events were used. In brief, the data analysis procedure includes the following primary steps. Reconstructed in TPCs global tracks having momentum and dE/dx information are extrapolated to the TOF detector wall and ascribed with the mass squared value m^2 derived from the time-of-flight measurement. In furhter, only those tracks are accepted for analysis which have a single hit in the individual scintillator pixel of TOF detector, i.e. double hits, conversion pairs from gammas in scintillator pixels are rejected from the analysis. The corresponding efficiency corrections have been applied to the data. The tracks are then subjected to the identification cuts upon dE/dx and m^2 values in order to select those identified as the deuteron or proton and to reject the pions and most of the kaons optimizing the rate of deuterons(protons) and minimizing the background contribution mostly coming from the other charged particles. The correction factors for the deuteron(proton) loss and some residual background contamination due to the cuts were estimated from experimental distributions.

The centrality samples of Pb+Pb collisions are selected subdividing the forward energy E_{zdc} measured in zero degree calorimeter ZDC into six bins. In each centrality bin, a direct estimate of interacting or participating nucleons N_{part} is made by calculating the net baryon number carried by all particles emitted from the collision into phase space region other than the spectator region [22]. For this calculation, the charged particle spectra measured in almost full forward hemisphere acceptable in the NA49 experiment with only small extrapolation to beam rapidity were used [23,24]. Here, a scaling factors determined from VENUS and RQMD event generators are employed to relate N_{part} to the measured yields of the net protons and charged kaons used in calculations. The second approach uses an estimate of the number of spectators in an event via a direct measure of the energy deposited in ZDC by projectile spectator nucleons. This method relies on both the event generation and GEANT detector simulation of ZDC response. Above estimetes of N_{part} from the measured final spectra) and the energy in ZDC agree well and considered reasonable bounds on the true mean $\langle N_{part} \rangle$ for each centrality sample used in the analysis. The estimate of impact parameter b is also based on the E_{zdc} measurement through the correlation of b with the energy in calorimeter produced by events simulated at fixed b by an event generator. The collision centrality parameters are summarised in Table 1.

Table 1. Pb+Pb centrality bins from most central (1) to peripheral (6). Columns show the E_{cal}/E_{beam} range, the covered range in fraction of the total cross section σ_{tot}, the mean number of participating nucleons $\langle N_{part} \rangle$ and the impact parameter b range for the corresponding cross sections.

Centrality bin	E_{cal} / E_{beam}	Fraction of σ_{tot}(%)	$\langle N_{part} \rangle$	b Range (fm)
1	0 - 0.25	0-5	366 ± 8	0-3.4
2	0.25 - 0.40	5-12	309 ± 10	3.4-5.3
3	0.40 - 0.58	12-23	242 ± 10	5.3-7.4
4	0.58 - 0.71	23-33	178 ± 10	7.4-9.1
5	0.71 - 0.80	33-43	132 ± 10	9.1-10.2
6	0.80 - 1.00	43-100	85 ± 6	10.2-14.0

The identified protons are contaminated by protons from weak decays of strange baryons that were incorrectly reconstructed as a tracks from primary vertex. They must be subtracted from the proton spectra in order to obtain the proton distributon from primordial interactions, i.e. the proton distibutions at freeze-out. This background correction was assessed using a GEANT-based Monte Carlo simulation of the decay of Λ and Σ hyperons and reconstruction of their charged decay products.

For generating representative phase space distributions of the decaying baryons the recent results from the SPS experiments WA97/NA57 [27] and NA49 [28] on the Λ production, including those from Σ^0-decays, have been used. A small fraction of protons from Σ^+-decays was calculated using the RQMD2.3 model simulation.

The overall contribution of feed-down protons was found to be 20-25% and almost independent on the collision centrality. Since an experimental data are majorly used this estimation gives a fair account of the proton feed-down correction introducing relatively small systematic errors of about 5-10% slightly dependending on the collision centrality.

Geometrical acceptance correction of the data was done by means of the Monte Carlo simulation of the detector in GEANT. The track reconstruction efficiency was determined by simulation using the method of embedding the tracks into real events. The tracking efficiency was estimated to be closer to 100% in the kinematical range limited by the TOF acceptance.

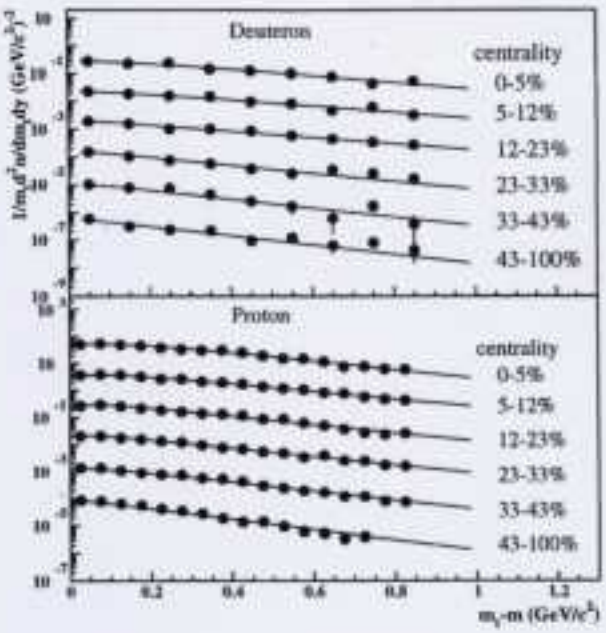

FIG. 2. Transverse mass distributions for deuterons in rapidity bin $2.0 < y < 2.5$ and for protons in rapidity bin $2.4 < y < 2.8$ measured at various centralities of 158 AGeV Pb+Pb collisions. The curves through the measured poins represent fits to Eq.(2). The fit parameters are listed in Table 2. The spectra are scaled down by a factor of 10 successively from upper one corresponding to the 0-5% centrality cut.

After all corrections, the transverse mass ($m_t = \sqrt{p_t^2 + m^2}$, m - particle mass) distributions for deuteron and proton were obtained (Fig.2).

The m_t-distributions were fitted with the function composed of two exponentials:

$$\frac{d^2N}{m_t dm_t dy} = C_1 e^{-(m_t - m)/T_1} + C_2 e^{-(m_t - m)/T_2}, \quad (2)$$

one of them describing the large m_t behaviour and the other one a deficit at small m_t. This expression is found to describe the data well, especially in central interactions where the particle yield at low m_t is suppressed relative to an exponential distribution of the Boltzmann type. The inverse slopes T were obtained from the exponential fits for m_t above the values where these deviations are not seen ($m_t - m > 0.2 - 0.3$ GeV/c^2). The numerical parameters for the inverse slope T and the particle yield dn/dy are tabulated in Table 2. The last were obtained by integrating the parametrized fit function over the full m_t range. The errors quoted in Table 2 are statistical.

The sources of systematic uncertainties are considered include possible errors in the determination of the efficiency corrections as discussed above, in particular those for selection of a single tracks in the TOF pixels as well as for particle identification and background subtraction. The last is particularly relevant to the deuterons at the highest momenta and the most peripheral bins repre-

sented with relatively poor statistics. For protons, a systematic error is additionally contributed on account of the feed-down corrections. An estimation of the particle yield dn/dy represents extrapolation into unmeasured regions under the explicit assumption of a certain shape of the m_t distribution. The inverse slope parameter T depends on which range the data are fitted, because the data do not exactly follow the assumed functional form. For the deuteron results, the systematic errors have not been contributed substantially as compared to statistical errors resulting in the total errors for the inverse slope T to be 40-50 MeV, almost independent on centrality, and for the particle yield dn/dy to vary from 15 to 30% in central and peripheral bins, respectively. The overall uncertainty of the proton results are about equally contributed by the statistical and systematic errors and estimated to be approximately 15 MeV for T and for dn/dy getting slightly increased from 5 to 10% when going from the most central to peripheral bins.

Table 2. Inverse slope T and particle yield dn/dy for deuterons ($2.0 < y < 2.5$) and protons ($2.4 < y < 2.8$) at various centralities in 158 AGeV Pb+Pb collisions. The errors are statistcal.

Centrality (% of σ_{tot})	T_d (MeV)	dn_d/dy	T_p (MeV)	dn_p/dy
0-5	425 ± 39	0.32 ± 0.03	308 ± 9	29.6 ± 0.9
5-12	421 ± 44	0.26 ± 0.03	308 ± 9	22.2 ± 0.6
12-23	416 ± 38	0.21 ± 0.03	276 ± 9	14.5 ± 0.4
23-33	330 ± 33	0.12 ± 0.02	273 ± 10	9.8 ± 0.3
33-43	279 ± 28	0.08 ± 0.01	245 ± 10	5.7 ± 0.2
43-100	279 ± 35	0.04 ± 0.01	216 ± 10	2.9 ± 0.1

The transverse mass distributions are at 40 and 80 AGeV beam energies for the 7% most central Pb+Pb collisions which corresponds to the mean number of participating nucleons $\langle N_{part} \rangle$=349. The data are measured just close to midrapidity, namely in the rapidity range of $1.8 < y < 2.3$ for protons and $1.9 < y < 2.3$ for deuterons at 40 AGeV (y_{cm}=2.22), and $1.8 < y < 2.3$ for protons and $2.1 < y < 2.5$ for deuterons at 80 AGeV (y_{cm}=2.56). The number of analised events was about 400,000 for 40 AGeV and 300,000 for 80 AGeV. Analysis of the data have been performed similarly to that of 158 AGeV energy including the proton feed-down correction. For this the NA49 results [28] on the Λ production at 40 and 80 AGeV Pb+Pb interactions obtained from the same data samples were used.

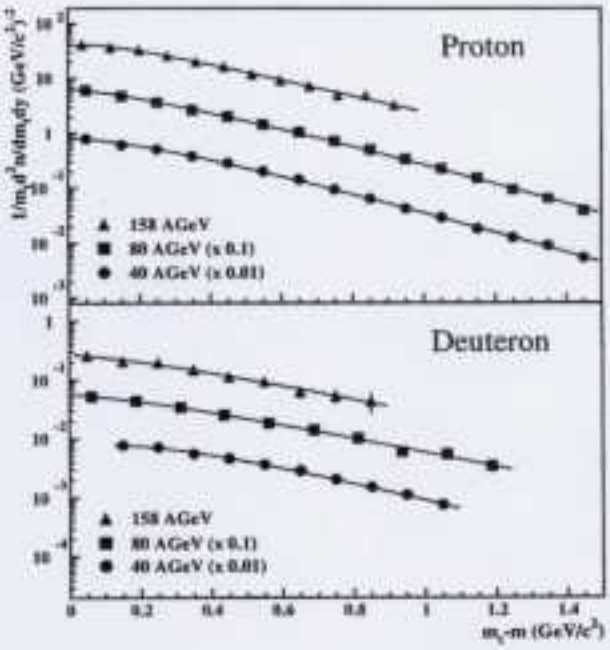

FIG. 3. Transverse mass distributions for deuterons and protons near midrapidity in central Pb+Pb collisions at 40, 80 and 158 AGeV. The solid lines illustrate two exponential fit to the data. The fitted parameters are listed in Table 3.

Fig.3 depicts the deuteron and proton m_t-spectra for all three energies together with a double exponential function fitted to the data. Again, an obvious deviation from single exponential shape is seen. The numerical values of the inverse slopes T and particle yields dn/dy are listed in Table 3 which have been obtained in the same manner as those in above analysis of the 158 AGeV data.

Table 3. Inverse slope T and particle yield dn/dy for deuterons and protons in cental Pb+Pb collisions at 40, 80 amd 158 AGeV beam energies E_{beam}. For completeness, the yields at 11.7 AGeV Au+Au collisions are also shown. The errors are statistcal.

E_{beam} (AGeV)	T_d (MeV)	dn_d/dy	T_p (MeV)	dn_p/dy
158	425 ± 39	0.32 ± 0.03	308 ± 9	29.6 ± 0.9
80	360 ± 15	0.59 ± 0.04	260 ± 11	30.1 ± 1.0
40	339 ± 9	1.02 ± 0.05	257 ± 11	41.3 ± 1.1
11.7 *)	-	5.00 ± 0.50	-	60.0 ± 1.5

*) Ref. [12], E-802 Collaboration

IV. DISCUSSION

The transverse mass spectra for deuterons in Pb+Pb collisions at 158 AGeV are observed to be significantly harder than those for protons, especially in central collisions. This is illustrated in Fig.4 where the inverse slopes T and the average transverse momenta $\langle p_t \rangle$ are plotted as a function of the number of participating nucleons N_{part}. To obtain $\langle p_t \rangle$ averaged over full kinematical range, an extrapolation to high p_t must be made. This extrapolation is typically some less than 10% and 20% for protons and deuterons, respectively, and done by fitting the measured spectra by Eq.(2) which, as discussed early, fits the spectra well. For all centralities, T and $\langle p_t \rangle$ is larger for deuterons and this effect is most pronounced in central collisions. The difference in T approaches zero more rapidly than the difference in $\langle p_t \rangle$. This indicates that the low p_t effects observed in the deuteron and proton distributions are less dependent on the system size than the high p_t spectral shape. It is also seen, that inverse slopes of the deuterons and protons decrease with diminishing centrality converging at approximately single value of $T \simeq 200$ MeV in the most peripheral points.

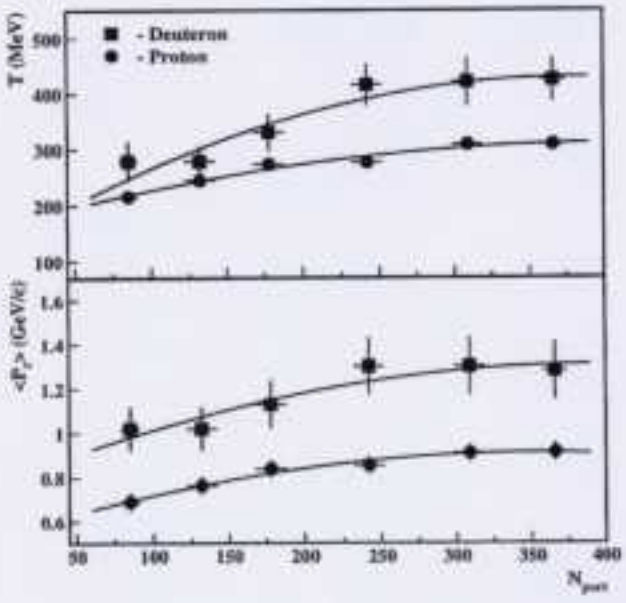

FIG. 4. Inverse slope parameter T and average transverse momentum $\langle p_t \rangle$ for deuterons in the rapidity range $2.0 < y < 2.5$) and for protons at $2.4 < y < 2.8$) as a function of the estimated N_{part} in 158 AGeV Pb+Pb collisions. Overlaid on the points are the polinomial fits to underline the trend. The errors are statistical.

From central data at 40, 80 and 158 AGeV, there is a clear evidence that the m_t-spectra for both deuterons and protons get flatter with increasing the incident energy. Also, an obvious deviation from a single exponential at small m_t, so called 'shoulder-arm' shape of the transverse mass distributions discussed, for example in [34], is hold for all three energies.

Above observations, an increase with mass of the inverse slope parameter and deviation of the m_t-spectra from an exponential distribution at small transverse mass as well as the evolution of these features with centrality and beam energy are the predicted characteristics of collective flow [29,37], which are expected to be stronger in central rather than peripheral collisions, similarly to what is observed in the measurement.

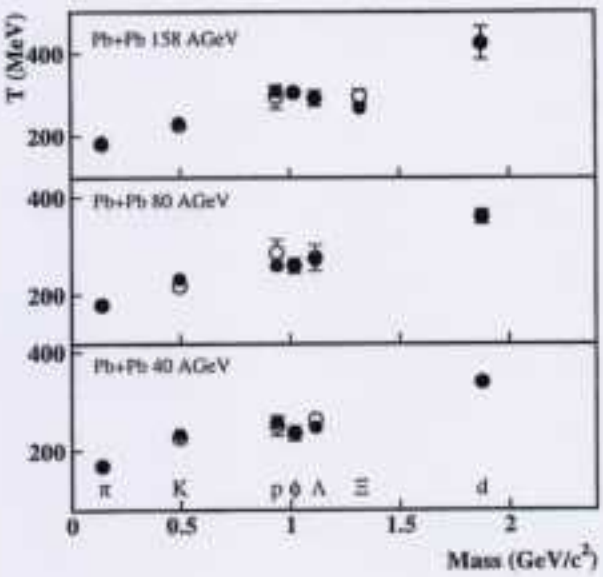

FIG. 5. Inverse slope parameters T for various particle species measured by NA49 near midrapidity in central Pb+Pb collisions at 40, 80 and 158 AGeV beam energies. Solid and open points are for for particle and antiparticles respectively. The data for π^- and $K^\pm$ are from Ref. [43], Λ and Ξ baryons are from Ref. [28] and [44,45], respectively, for ϕ mesons are from Ref. [46], whereas the results for p and d are obtained in this work. The quoted errors are statistical.

The study of transverse mass spectra at the top SPS energy has been carried out by several experiments and it was realized that the inverse slope T of the transverse mass distribution increases steadily with the mass of the considered particle (for review see [42]). This was explained as arising from the relativistic superposition of the expanding system plus a radial collective flow [30,37,48].

The present data together with those recently obtained by NA49 [28,43–45] extended the results on a mass systematics of inverse slope to the lower region of SPS energy and for various species of emitted particles, from pions to deuterons, which are depicted in Fig.5. The study is performed with identical experimental apparatus, thus largely eliminating possible systematic uncertainty in comparing different energies. The previous observations on the inverse slope parameters in central Pb+Pb collisions at 158 AGeV as increasing with increasing a mass of emitted particles is further supported

by the measurements at 40 and 80 AGeV beam energies. It is also seen from the figure, that the inverse slopes for light particles, π^- and $K^\pm$, show no visible variation with beam energy , at least within the errors, whereas, for heavier species, p, d, Λ, and ϕ, the inverse slopes exhibit systematic increase with increasing the beam energy even at the SPS energy range.

The deuteron measurement together with the mesurement of protons allows for the determination of the deuteron coalescence parameters B_2 which can be calculated from our data applying a generalized Eq.(1) for the produced cluster of A=2 .

The measured quantities of B_2 at small p_t close to zero in rapidity bin $2.0 < y < 2.5$ versus the number of participating nucleons N_{part} are plotted at the top pannel of Fig.5 along with a comparative data deduced from the NA52 experiment [15]. Numerical values of B_2 are tabulated in Table 4.

Table 4. Coalescence parameter B_2 at nearly zero p_t for six centrality bins specified by the mean numbers of participating nucleons $\langle N_{part} \rangle$. The estimated total errors are quoted .

$\langle N_{part} \rangle$	85	132	178
$B_2 \cdot 10^4$ (GeV$^2/c^3$)	32.0 ± 9.0	27.0 ± 8.0	16.0 ± 4.0
$\langle N_{part} \rangle$	242	309	366
$B_2 \cdot 10^4$ (GeV$^2/c^3$)	10.0 ± 2.5	6.5 ± 1.5	4.5 ± 1.0

Being in a good consistency, the results show that the coalescence parameter in the most central Pb+Pb interactions ($B_2 \simeq 4.5 \cdot 10^{-4}$ GeV$^2/c^3$) is nearly one-tenth of that measured close to the most peripheral points exhibiting a strong centrality dependence. Similarly to the interpretation of the drastic drope in B_2 at higher energies, the observed centrality dependence of B_2 also may imply a changing effective freeze-out volume of the emission sorce arising from the dynamics of the expansion.

The B_2 parameter may be related through the coalescence models to the size of the particle emission source [3–5]. As the dynamics of the collisions is belived to be important for the coalescence mechanism we followed the model by Scheibl and Heinz [19] that explicitly consider rapid collective expansion of the collision zone. The model includes the effect of collective flow in a density matrix approach for coalescence and results in a connection between the B_2 and the volume of homogeneity (the interaction volume) as $B_2 \propto 1/(R^2_{side} \cdot R_{long})$ given by equations (6.3) and (6.4) of Ref. [19]. The terms R_{side} and R_{long} are the transverse and longitudinal dimensions of the emission source at freeze-out which are comparable to those extracted from HBT interferometry.

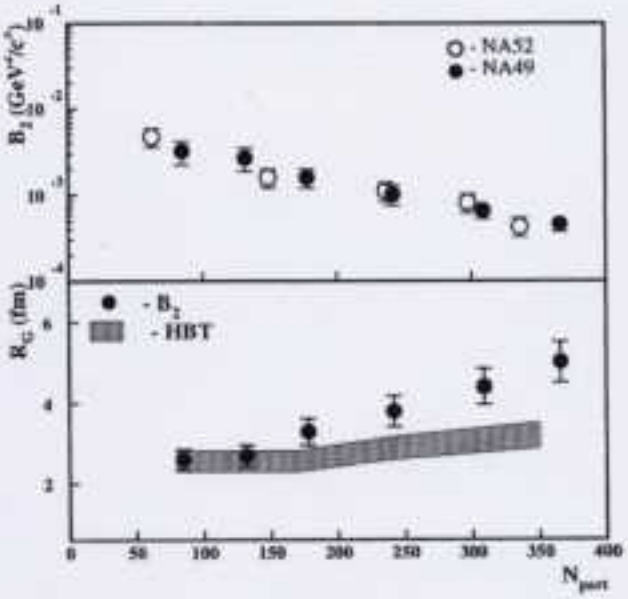

FIG. 6. Top: Deuteron coalescence factor B_2 in 158 AGeV Pb+Pb collisions near zero p_t and rapidity interval $2.0 < y < 2.5$ is illustrated as a function of the number of participating nucleons N_{part} and compared to the result of the NA52 measurement [15] at y=3.7 (y=2.1 reflected at midrapidity y_{cm}=2.91). Bottom: Source radius parameter R_G extracted from the measured B_2 in the context of the coalescence model [19] and from the HBT data of NA49 for correlations of $\pi\pi$ [39], KK [41] and pp [40] pairs shown as shaded bands indicating the estimated systematic errors.

Using the prescription of the model and our results on B_2 we extracted radius parameter of the system R_G for each centrality bin written as $R_G = (R^2_{side} \cdot R_{long})^{1/3}$ which are displayed in the bottom panel of Fig.6 by a solid points. The radius parameter R_G as a function of N_{part} derived from the recent HBT results of NA49 is also presented in the figure as a shaded bands specifying the estimated uncertainty of the data. It is important to note, as the source size extracted in the context of the coalescence model corresponds to setting m_t=m_N, the radius parameters R_{side} and R_{long} used for comparison should also be relative to similar m_t value in the HBT case.

For this calculations, the radius parameters measured for pion-pairs at $m_t = 0.2$ GeV$/c^2$ for various N_{part} were corrected to the m_t value nearly equal to nucleon mass. The latter was done employing the m_t distribution of the parameter R_G derived from combined anaalysis of the correlation data for $\pi\pi$ [39], KK [41] and pp [40] pairs in central 158 AGeV Pb+Pb collisions. Above m_t distribution is in a good consistency with the NA44 results [49].

It is observed from the data, that the radius parameter derived from the coalescence data is rather consistent with those from HBT results in peripheral and mid-central Pb+Pb collisions, while approaching to the central interactions it increases steeper getting about two times larger than that from HBT.

There is another hint on possible discrepancy between the coalescence and HBT calculations of the source size. Namely, the difference in B_2 in central Pb+Pb collisions at 40 and 158 AGeV, to be shown, accounts for about 30% difference in the R_O value, which is however not seen in the HBT case [39].

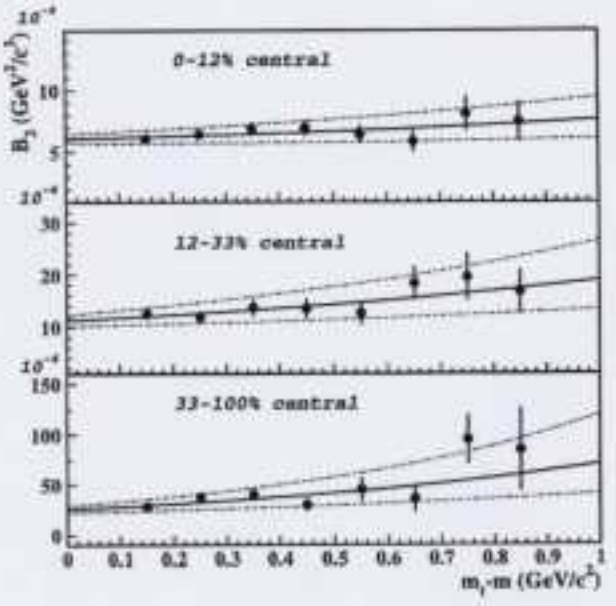

FIG. 7. Coalescence factor B_2 for 158 AGeV Pb+Pb reaction as a function of the deuteron transverse mass $m_t - m$ for three sets of centrality cuts. Shown overlaid on the points are curves of the exponential fit of the functional form $B_2(m_t)$=a · exp(b($m_t - m$)). The dotted lines represent the effect of the $\pm 1\sigma$ errors of the fitted parameter b. The error bars are statistical.

Dependence of the coalescence parameter B_2 on the deuteron transverse mass $m_t - m$ is displayed in Fig.6 for three centrality regions covering (0-12)% , (12-33)% and (33-100)% of σ_{tot}. The solid lines overlaid on the points are the exponential fit of the functional form $B_2(m_t) = a \cdot exp(b(m_t - m))$. The figure demonstrates that the coalescence probability B_2 increases at large m_t values in each of three centrality selected data samples. In the meantime, while the first two more central bins represent reasonably exclusive cuts on event geometry, the third more peripheral bin represents the events averaged over a large range in collision geometry. However, it is belived that in a far reaching peripheral collisions there will be no m_t dependence of B_2, a feature expected because of the difference in inverse slopes for deuterons and protons approaches to zero, as it is evident in Fig.4.

It should be noted that the proton and deuteron distributions used for B_2 calculations at 158 AGeV are measured not exactly in similar but partially overlaped rapidity intervals. It introduces some uncertainty which is estimated using the data [22–24] to be rather small entirely contained within the quoted systematic errors for B_2. To give the numerical values: if the proton data at rapidity $2.4 < y < 2.8$ are corrected to the rapidity interval of the deuteron measurements $2.0 < y < 2.5$, the proton yield dn/dy increases by nearly 5% and the inverse slope systematicaly decreases by 10-15 MeV at most , and this results in approximately 10% reduction in B_2 at small m_t values and slightly steeper increase with m_t getting about 10% growth at $m_t - m = 1.0$ GeV/c^2.

In the recent models [18,19] that consider strong collective expansion the cluster spectra and the coalescence parameters were calculated for various functional forms of nucleon density and transverse expansion velocity. From these study, the increase in B_2 with transverse mass and larger inverse slope for deuterons than for protons observed in the experiment well consistent with a constant transverse density distribution of the source at freeze-out, which is closer to a box than a Gaussian shape, and with a linear radial flow velocity profile.

The B_2 values measured at 40, 80 and 158 AGeV beam energies for central Pb+Pb collisions are displayed in Fig.8. A comparative data measured at the other energies are also shown. A repeatedly reviewed feature of decrease in B_2 with increasing beam energy is supported by the present measurements exhibiting a continuos rise of B2, at least by a factor of 2, when going from the top SPS energy to the energies of AGS.

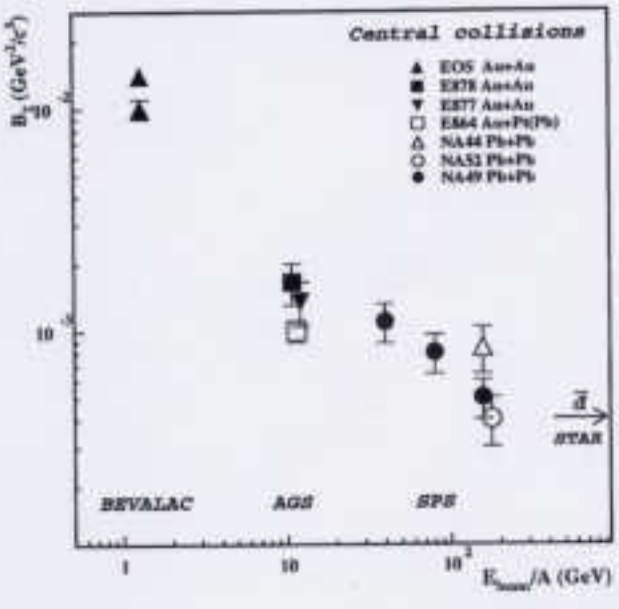

FIG. 8. Coalescence factor B_2 for central Pb+Pb collisions at 40, 80 and 158 AGeV beam energies reviewed together with those from the Bevalac [8], AGS [10,11,14] and SPS [15,16]. The data for central collisions of heavy systems measured near midrapidity are only used. The result for anti-deuterons from the RHIC measured by STAR [38] is also quoted.

V. SUMMARY

In central 158 AGeV Pb+Pb collisions near midrapidity the deuteron inverse slope ($T_p \simeq 420$ MeV) is considearably greater than the slope for protons ($T_p \simeq 310$ MeV), while in most peripheral collisions they both decrease converging at about $T_{d,p} \simeq 200$ MeV. The spectra show a deviation from an exponential behaviour at small m_t which is most pronounced in central bins rather than peripheral These features are also valid for deuteron and proton m_t spectra in central Pb+Pb reactions at 40 and 80 AGeV incident energies.

The coalescence factor in most central bin is estimated to be $B_2 \simeq 4.5 \cdot 10^{-4}$ GeV$^2/c^3$, and it increases by about an order of magnitude when approaching to the most peripheral collisions, by this exhibiting a strong dependence on the system size of the collision. The coalescence parameter B_2 shows the trend of increasing at large transverse mass m_t. The observed increase in B_2 with transverse mass supports the (conclusion)(prediction) that the emission source (nucleon density profile)(the radial density profile of the nucleon source) is closer to the box shape with a sharp surface, and the transverse expansion velosity profile is nearly linear. The B_2 steadily decreases with increasing the beam energy in the range between AGS and SPS top energies.

The radius parameter of the particle emission source R_G derived from the B_2 measurement is satisfactory consistent to that from Bose Einstein correlations in peripheral and mid-central Pb+Pb collisions while approaching to central collisions it rises steeper than radius obtained from the correlation analysis. The radius parameter obtained from the HBT data changes less with centrality than radius derived from the B_2 measurements in the context of the coalescence model.

In general, above observations are consistent with the features predicted by models that include in consideration the presence of a strong collective expansion in heavy ion nucleus-nucleus collisions.

VI. ACKNOWLEDGEMENTS

This work was supported by the Director, Office of Energy Research, Division of Nuclear Physics of the Office of High Energy and Nuclear Physics of the US Department of Energy (DE-ACO3-76SFOOO98 and DE-FG02-91ER40609), the US National Science Foundation, the Bundesministerium fur Bildung und Forschung, Germany, the Alexander von Humboldt Foundation, the UK Engineering and Physical Sciences Research Council, the Polish State Committee for Scientific Research (2 P03B 130 23 and 2 P03B 02418), the Hungarian Scientific Research Foundation (T14920 and T32293), Hungarian National Science Foundation, OTKA, (F034707), the EC Marie Curie Foundation, and the Polish-German Foundation.

[1] Proc. Quark Matter'99, Nucl. Phys. **A661** (1999); Proc. Quark Matter'2001, Nucl. Phys. **A698** (2002).
[2] L.P.Csernai and J.I.Kapusta, Phys. Rep. **131**, 223 (1986).
[3] A.Mekjian, Phys. Rev. Lett. **38**, 640 (1977); S.Das Gupta and A.Z.Mekjian, Phys. Rep. **72**, 131 (1981).
[4] H.Sato and K.Yazaki, Phys. Lett. B **98**, 153 (1981).
[5] R.Bond *et al.*, Phys. Lett. B **71**, 43 (1977)
[6] S.T.Butler and C.A.Pearson, Phys. Rev. **129**, 836 (1963); A.Schwarzschild and Č.Zupančič, Phys. Rev. **129**, 854 (1963).
[7] H.H.Gutbrod *et al.*, Phys. Rev. Lett. **37**, 667 (1976); M.-C.Lemaire *et al.*, Phys. Lett. B **85**, 38 (1979); S.Nagamiya *et al.*, Phys. Rev. C **24**, 971 (1981); R.L.Auble *et al.*, Phys. Rev. C **28**, 1552 (1983).
[8] S.Wang *et al.*, Phys. Rev. Lett. **74**, 2646 (1995).
[9] J.W.Cronin *et al.*, Phys. Rev. D **11**, 3105 (1975); W.Bozzoli *et al.*, Nucl. Phys. B **144**, 317 (1978).
[10] J.Barrette *et al.*, Phys. Rev. C **50**, 1077 (1994); T.Abbott *et al.*, Phys. Rev. C **50**, 1024 (1994); N.Saito *et al.*, Phys. Rev. C **49**, 3211 (1994).
[11] M.J.Bennett *et al.*, Phys. Rev. C **58**, 1155 (1998).
[12] L.Ahle *et al.*, Phys. Rev. C **60**, 064901 (1999).
[13] J.Barrette *et al.*, Phys. Rev. C **61**, 044906 (2000).
[14] T.A.Armstrong *et al.*, Phys. Rev. C **61**, 064908 (2000).
[15] G.Ambrosini *et al.*, New J. Phys. **1**, 22.1 (1999).
[16] A.G.Hansen *et al.*, Nucl. Phys. **A661**, 387c (1999).
[17] S.V.Afanasiev *et al.*, Phys. Lett. B **486**, 22 (2000).
[18] A.Polleri *et al.*, Phys. Lett. B **419**, 19 (1998); Phys. Lett. B **473**, 193 (2000).
[19] R.Scheibl and U.Heinz, Phys. Rev. C **59**, 1585 (1999).
[20] J.L.Nagle *et al.*, Phys. Rev. C **53**, 367 (1996).
[21] S.Afanasiev *et al.*, Nucl. Instrum. Methods Phys. Res. A **430**, 210 (1999).
[22] G.E.Cooper *et al.*, Nucl. Phys. **A661**, 362c (1999).
[23] F.Siklér *et al.*, Nucl. Phys. **A661**, 45c (1999).
[24] H.Appelshäuser *et al.*, Phys. Rev. Lett. **82**, 2471 (1999).
[25] K.Werner, Phys. Rep. **232**, 87 (1993).
[26] H.Sorge, Phys. Rev. C **52**, 3291 (1995).
[27] R.A.Fini *et al.*, J. Phys. G: Nucl. Part. Phys. **27**, 375 (2001).
[28] A.Mischke *et al.*, J. Phys. G: Nucl. Part. Phys. **28**, 1761 (2002).
[29] H.Sorge, J.L.Nagle and B.S.Kumar, Phys. Lett. B **355**, 27 (1995); J.Sollfrank *et al.*, Z. Phys. C **52**, 593 (1991); U Heinz, Nucl. Phys. **A610**, 264c (1996).
[30] G.Roland *et al.*, Nucl. Phys. **A638**, 91c (1998).
[31] U.Heinz *et al.*, Phys. Lett. B **382**, 181 (1996); S.Chapman, J.R.Nix and U.Heinz, Phys. Rev. C **52**, 2694 (1995).
[32] W.Llope *et al.*, Phys. Rev. C **52**, 2004 (1995); B.Monreal *et al.*, Phys. Rev. C **60**, 031901 (1999).
[33] R.Bond et al., Phys. Lett. B **71**, 43 (1977).

[34] L.Ahle et al., Phys. Rev. C **57**, R466 (1998).
[35] R.Mattiello, H.Sorge, H.Stocker, and W.Greiner, Phys. Rev. C **55**, 1443 (1997).
[36] T.Alber *et al.*, Phys. Rev. Lett. **75**, 3814 (1995); H.Appelshäuser *et al.*, Eur. Phys .J. A **2**, 383 (1998).
[37] P.Braun-Munzinger, J.Stachel, J.P.Wessels and N.Xu, Phys. Lett. B **344**, 43 (1995); H.Appelshäuser *et al.*, Eur. Phys. J. C **2**, 661 (1998); E.Schnedermann, J.Sollfrank and U.Heinz, Phys. Rev. C **48**, 2462 (1993).
[38] C.Adler *et al.*, Phys. Rev. Lett. **87**, 262301 (2001).
[39] C.Blume *et al.*, nucl-ex/0208020; to appear in Nucl. Phys. A (2003).
[40] H.Appelshäuser *et al.*, Phys. Lett.B **467**, 21 (1999).
[41] S.V.Afanasiev *et al.*, to appear in Phys. Lett. B (2003).
[42] J.B.Kinson, J. Phys. G: Nucl. Part. Phys. **25**, 143 (2001).
[43] S.V.Afanasiev *et al.*, Phys. Rev. C **66**, 054902 (2002).
[44] S.V.Afanasiev *et al.*, Phys. Lett. B **538**, 275 (2002).
[45] S.V.Afanasiev *et al.*, Phys. Lett. B **444**, 523 (1998).
[46] S.V.Afanasiev *et al.*, Phys. Lett. B **491**, 59 (2000).
[47] A.Mischke *et al.*, nucl-ex/0209002; to appear in Nucl. Phys. A (2003).
[48] I.G.Bearden*et al.*, Phys. Rev. Lett. **76**, 2080 (1997).
[49] I.G.Bearden*et al.*, Phys. Rev. Lett. **87**, 112301 (2001).